The proteasome load versus capacity balance determines apoptotic sensitivity of multiple myeloma cells to proteasome inhibition

UNIVERSITÀ DEGLI STUDI DI TORINO

The proteasome load versus capacity balance determines apoptotic sensitivity of multiple myeloma cells to proteasome inhibition

*Giada Bianchi,1-3 *Laura Oliva,1,4 Paolo Cascio,5 Niccolo` Pengo,1,2,4 Francesca Fontana,1,2,6 Fulvia Cerruti,5 Andrea Orsi,1,2 Elena Pasqualetto,1,4 Alexandre Mezghrani,7 Valeria Calbi,4,8 Giovanni Palladini,9 Nicola Giuliani,10 Kenneth C. Anderson,3 †Roberto Sitia,1,2,4 and †Simone Cenci1,2,4,6

1Division of Genetics and Cell Biology, San Raffaele Scientific Institute, Milano, Italy; 2Universita` Vita-Salute San Raffaele, Milano, Italy; 3The LeBow Institute for Myeloma Therapeutics and Jerome Lipper Center for Myeloma Research, Department of Medical Oncology, Dana-Farber Cancer Institute, Harvard Medical School, Boston, MA; 4Myeloma Unit, San Raffaele Scientific Institute, Milano, Italy; 5Department of Veterinary Morphophysiology, University of Torino, Torino, Italy; 6BoNetwork, San Raffaele Scientific Institute, Milano, Italy; 7Institut de Ge´nomique Fonctionnelle, Centre National de la Recherche Scientifique (CNRS), Montpellier, France; 8Hematology and Bone Marrow Transplantation (BMT) Unit, San Raffaele Scientific Institute, Milano, Italy; 9Amyloidosis Center, Biotechnology Research Laboratories, Fondazione Istituto di Ricovero e Cura a Carattere Scientifico (IRCCS) Policlinico San Matteo, Department of Biochemistry, University of Pavia, Pavia, Italy; and 10Hematology and BMT Center, University of Parma, Parma, Italy

Proteasome inhibitors (PIs) are effective against multiple myeloma (MM), but the mechanisms of action and bases of individual susceptibility remain unclear. Recent work linked PI sensitivity to protein synthesis and proteasome activity, raising the question whether different levels of proteasome expression and workload underlie PI sensitivity inMMcells (MMCs). Exploiting human MM lines characterized by differential PI sensitivity, we report that highly sensitive MMCs express lower proteasome levels and higher proteasomal workload than relatively PI-resistant MMCs, resulting in the accumulation of polyubiquitinated proteins at the expense of free ubiquitin (proteasome stress). Manipulating proteasome expression or workload alters apoptotic sensitivity to PI, demonstrating a cause-effect relationship between proteasome stress and apoptotic responses in MMCs. Intracellular immunostaining in primary, patientderived MMCs reveals that polyubiquitinated proteins hallmark neoplastic plasma cells, in positive correlation with immunoglobulin (Ig) content, both intra- and interpatient. Moreover, overall proteasome activity of primary MMCs inversely correlates with apoptotic sensitivity to PI. Altogether, our data indicate that the balance between proteasome workload and degradative capacity represents a critical determinant of apoptotic sensitivity of MMCs to PI, potentially providing a framework for identifying indicators of responsiveness and designing novel combination therapies.

Introduction

Multiple Myeloma (MM) is a frequent and still incurable plasma cell malignancy, causing 2% of all cancer deaths. In recent years, treatment of MM has improved remarkably. For example, the proteasome inhibitor (PI) bortezomib (PS-341, Velcade™) proved effective even in the context of heavily pretreated, relapsed and refractory MM 1-3, although > 50% patients fail to respond to second line treatment 4. The molecular bases of different individual responsiveness to bortezomib remain unclear. Age (< 65 years) and extent of bone marrow plasma cell infiltration (< 50%) are the conventional factors for successful treatment identified so far 5-7. Identifying the molecular bases underlying PI sensitivity would provide the framework for their improved clinical application.

Bortezomib targets the proteasome, a 2.4 MDa multicatalytic protease complex ubiquitously expressed in eukaryotic cells 1,8. Being crucial for degrading proteins involved in cell cycle, angiogenesis, adhesion, cytokine production, and apoptosis 3,9,10, proteasome inhibition can affect tumor cell growth via direct and indirect mechanisms, e.g. by blocking interactions with endothelial and bone cells 8,11. Proteasomes also dismantle damaged and misfolded/ unfolded proteins, potentially harmful for the cell 8. As a result, proteasome impairment causes buildup of poly-ubiquitinated proteins and eventual cell death 3. Proteasomes also degrade a significant proportion of newly synthesized proteins in mammalian cells (rapidly degraded polypeptides, RDP) 12. Thus, increased protein synthesis or other metabolic unbalances could increase proteasome workload.

We recently showed that plasma cell differentiation *in vitro, ex vivo*, and *in vivo* entails a dramatic decrease in proteasome expression and activity, correlating with increased sensitivity to PI 13,14. Indeed, PI reduce Ab responses *in vivo* 14,15. Moreover, inducible expression of orphan Ig-μ chains sensitizes non-lymphoid tumor cells to PI-induced toxicity 13. In MMC the levels of both Ig synthesis and retention correlate with apoptotic sensitivity to PI, and manipulating Ig synthesis alters sensitivity 16,17. Altogether, these data suggest that the exquisite sensitivity of certain MMC to PI could stem from decreased proteasomal capacity, increased proteasomal workload, or both (i.e. an adverse *load vs. capacity* ratio).

In this study we exploited MM lines with differential apoptotic sensitivity to PI to address if proteasome expression and degradative workload vary among different clones, and defined their role in determining apoptotic sensitivity to PI. Moreover, using primary patient-derived MMC, we revealed correlations between proteasome stress and PI sensitivity. By establishing a causal relationship between proteasome stress and PI sensitivity in MM, our data may provide the framework for testing novel pharmacological synergies aimed at exacerbating proteotoxicity, and for identifying prognostic indicators to predict responsiveness to bortezomib in MM patients.

Materials and methods

Cell cultures

Patient-derived MMC were purified from bone marrow aspirates by CD138 immuno-magnetic positive selection (Miltenyi Microbeads), upon obtainment of patient's informed consent. Negative fractions were cultured for up to 4 weeks to purify stromal cells, as described 18. The mouse B lymphoma cell line I.29μ+, the human MM lines U266, RPMI8226, KMS.18 and MM.1S, and primary MMC were cultured in RPMI media supplemented with 10% fetal calf serum (FCS), glutamax (1 mM), penicillin (100 U/ml) and streptomycin (100 μg/ml). HeLa cells were cultured in D-MEM supplemented as above.

Flow-cytometric analyses of apoptosis

Cells were treated and harvested as indicated, stained with FITC-conjugated

AnnexinV and propidium iodide as per manufacturer's instructions, and analyzed by FACScalibur (BD Biosciences). Patient-derived MMC were seeded 30,000 cells/well and treated for 24 hr as indicated. High-sensitivity assessment of apoptosis was obtained with LSRII (BD Biosciences).

Pulse-chase assays for intracellular protein degradation

I.29μ+ and MMC lines were incubated for 15 min in starvation medium (2% FCS, methionine and cysteine-free) at 37°C. Cells were then pulse-labeled with 50 μCi/ml Pro-mix [35S] (Amersham) for the indicated time, washed twice in PBS, resuspended and chased in complete media containing 2.5 mM cold methionine ± PI. Each timepoint consisted of triplicates of 106 cells each. At the end of the chase, supernatants were recovered and cells lysed in RiPA buffer. Lysates and supernatants from 10,000 cells were precipitated with 25% TCA. After 30 min on ice, samples were collected on glass fiber filters and analyzed in a liquid scintillation counter (Packard, Canberra Company).

Reverse Transcriptase PCR analyses

Total cellular RNA was extracted with Trizol and reverse-transcribed with Superscript II RT (Invitrogen). Splicing of XBP-1 mRNA [RefSeq: NM013842] was analyzed by PCR with primers flanking the 26b intron (5'-GGAGTTAAGACAGCGCTTGG; 5'-ACTGGGTCCAAGTTGTCCAG). PCR products derived from the spliced (s) and unspliced (u) XBP-1 mRNAs were resolved by electrophoresis on a 2.5% agarose gel and visualized by ethidium bromide staining. Levels of HSP70i were quantitated by real-time PCR (SybrGreen I, Roche) with the following primers: 5'-CAGGTGATCAACGACGGAGACA; 5'-GTCGATCGTCAGGATGGACACG, upon normalization by histone H3 (5'-GTGAAGAAACCTCATCGTTACAGGCCTGGT; 5'-CTGCAAAGCACCAATAGCTGCACTCTGGAA).

Proteasome activity assays

Proteasome activity was assessed in MMC extracts using fluorogenic peptides as described 13,19,20 21. Briefly, cells were sonicated in ice-cold buffer (50 mM Tris/HCl pH 7.5, 1 mM DTT, 0.25 M sucrose, 5 mM MgCl2, 0.5 mM EDTA, 2 mM ATP) and extracts prepared by centrifugation for 30min at 10,000g and 15min at 100,000g. Proteasome-specific peptidase activities were assayed by monitoring the production of 7-amino-4-methylcoumarin (amc) from the following fluorogenic peptides (Bachem, Bubendorf, CH): 100 μM Suc-LLVY-amc (for chymotrypsin-like), 500 μM Bz-VGRamc (for trypsin-like) and 100 μM Ac-YVAD-amc (for caspase-like activity) in 20 mM Tris-HCl pH 7.5, 1 mM ATP, 2 mM MgCl2, 0.2% BSA. Reactions were started by adding an aliquot of cellular extract and the fluorescence of released amc (excitation, 380 nm; emission, 460 nm) was monitored continuously at 37°C with a Carry Eclipse spectrofluorometer. Background activity (caused by nonproteasomal degradation) was determined by addition of the proteasome inhibitors MG132 (for chymotryptic and caspase-like activities) and □-lactone (for trypsin-like activity) at a final concentration of 10 μM and 20 μM respectively. Assays were calibrated using standard solutions of free fluorophores and the reaction velocities were calculated from the slopes of the initial linear portions of the curves. Substrate consumption at the end of incubation never exceeded 1%.

Immunoblot analyses

Immunoblot analyses of proteasomal subunits and proteasome-related factors were performed upon cell lysis in RiPA buffer as described 22. To detect ubiquitin (Ub) and Ub-conjugates, cells were lysed in 150 mM NaCl; 1% NP-40; 50 mM Tris HCl, ph 7.5. Extracts were resolved by electrophoresis, blotted, and probed with the following primary Ab: rabbit antisera against LMP2 (a kind gift of Dr. K. Tanaka, Tokyo

Metropolitan Institute of Medical Science, Tokyo, Japan); LMP7, MECL1, □3, □4, □5, □6 (Biomol international, Exeter, UK); X and Y (Boston Biochem, Cambridge, MA, USA); mouse monoclonal against Z (a kind gift of Prof. A.L. Goldberg, Harvard Medical School, Boston, MA, USA); and Ub (St.Cruz sc-8017). Densitometric analysis of bands was performed with a VersaDoc 1000 Imaging System (Bio-Rad Laboratories, Hercules, CA, USA).

Immunofluorescence

MMC were seeded on poly-L-lysine-coated slides, fixed with 3.7% formaldehyde and permeabilized with PBS 0.1% Triton X100. Cells were stained with monoclonal antibodies against Ub (Fk2), LMP2 (LMP2/13), LMP7 (LMP7-1) (Biomol, Exeter, UK), or rabbit anti-□or □antisera (Dako), rinsed in PBS and stained with Alexa Fluor 488 goat anti-mouse IgG or Alexa Fluor 546 goat anti-rabbit IgG antibody and Hoechst 331 (Molecular Probes Inc., Oregon, USA). Coverslips were observed on a DeltaVision workstation (Applied Precision, USA). Higher magnification images of primary MMC were deconvoluted with SoftWorx 3.5.0. Automated quantification of Fk2 fluorescence in Ig-L+ and Ig-L- nucleated cells was performed using the IN Cell Investigator Software (GE Helthcare).

Generation of UbG76V-GFP expressing MM lines

MM.1S and U266 cells were transduced using a lentiviral vector previously generated by us 13 (1 μg/ml) encoding GFP destabilized by fusion to a mutated uncleavable ubiquitin moiety (UbG76V-GFP) 23. As revealed by PI treatment and microscopy, the proportion of cells stably expressing the reporter was 100% and 60% in MM.1S and U266, respectively. Stable U266 expressants were sorted upon reversible proteasomal inhibition (FACSCalibur, BD Biosciences).

Statistic analyses

To compare average measures of proteasome activity and apoptosis, we adopted a two-tailed Student's *t*-test. For quantified immunofluorescent signals, an intensity threshold (5,000) was set to discriminate clonal plasma cells as Ig light chain (Ig-L) expressants, based on Ig-L intensity distribution. Pearson's Correlation coefficients (r) were calculated with Prism (Graphpad) to study the correlation between Ig-L and Fk2 signals intra- and inter-patient.

Results

Decreased proteasome expression in differentiating B-lymphocytes is associated with increased proteasomal workload and higher apoptotic sensitivity to PI

In previous studies, we have shown that B cells acquire apoptotic sensitivity to PI when stimulated to differentiate into Ig-secreting cells both *in vitro* and *in vivo*, correlating with reduced expression of functional proteasomes and reduced overall proteasome activity 13,14. To gain insight into the actual utilization of the remaining proteasomes, we measured the disappearance of TCA-insoluble newly made proteins that could be inhibited by PI in LPS-stimulated I.29μ+ cells by pulse-chase assays. Whilst in controls degradation proceeded linearly for four hours of chase, LPS stimulation increased significantly the fraction of proteins degraded by proteasomes within 1 hour of chase, approaching 30% at day 3 (Fig. 1A), upon exit from the cell cycle and acquisition of an Ig-synthesizing phenotype 13. Therefore, the amount of proteins undergoing proteasomal degradation soon after synthesis was ~6 times higher in LPS-stimulated cells. This dramatic change could reflect the quantitative and qualitative proteomic and metabolic changes linked to B cell differentiation 24. Whatever their origin 12, these RDPs represent an increased load for the diminishing pool of proteasomes. In line with the stabilization of certain proteasome substrates

(e.g. XBP-1, IkB□, Bax) in differentiating I.29μ+ cells 13, after the initial phase of rapid degradation, the loss of TCA-insoluble radioactivity was slower in activated cells (Fig. 1A), probably reflecting reduced availability of proteasomes, fewer and actively degrading RDPs 13. The enhanced synthesis of longer-lived proteins, such as ER chaperones, and the possible re-utilization of radioactive amino acids generated by degradation could contribute to a slower second-phase degradation in LPS-activated cells. Shorter chase times revealed that the first phase in LPS-activated cells was essentially completed in the first 15 minutes of chase, with 27.5 % of RDPs having been already degraded (Fig. 1B). These data demonstrate that Ig-synthesizing cells display higher proteasome-mediated degradation of short-lived polypeptides, imposing a higher workload on decreased proteasome levels 13. This correlated with increased apoptotic sensitivity to bortezomib (Fig. 1C) and other PI 13, supporting a causative role for an unfavorable proteasomal workload vs. capacity ratio in predisposing to PI toxicity.

Decreased proteasome activity in PI-sensitive MMC

According to the load vs. capacity model, cells equipped with fewer proteasomes, higher workload, or both, should be more vulnerable to the toxic effects of bortezomib. Given the exquisite sensitivity of MMC to bortezomib and the importance of this drug in MM therapy, we decided to challenge our model in MMC. When challenged with bortezomib for 48 hours, the MM cell lines KMS.18 and MM.1S proved ~10 times more sensitive than U266 and RPMI8226, with the following EC50 values: ~4 nM for MM.1S cells, ~6 nM for KMS.18, ~46 nM for RPMI8226 and ~55 nM for U266 (Supplementary Fig. 1). When challenged with other PI, similar differences were observed, with MM.1S cells showing 5 and 10 times higher sensitivity than RPMI8226 or U266 to epoxomicin and MG-132, respectively. Next, to determine overall proteasome capacity, we assessed 26Sspecific peptidase activities in cellular extracts both per protein content (Fig. 2A) and per cell (not shown). In line with other reports on lymphoid cells 25, the chymotryptic activity accounted for 80%, and the caspase-like activity accounted for only 2% of all proteasome specific activity. While RPMI8226 had similar chymotryptic activity (79%), the highly sensitive lines KMS.18 and MM.1S displayed significantly lower chymotryptic activity than U266 (44.2 and 28%, respectively). Similarly, the trypsinlike activity of RPMI8226 cells was close (83%) to that of U266 cells, while it was significantly lower in KMS.18 and MM.1S cells (respectively 43% and 57% of U266). Finally, also the minor caspase-like activity was significantly lower than U266 in KMS.18 (44%) and slightly, but consistently in MM.1S cells (90%) (Fig. 2A).

To confirm that MM.1S and KMS.18 cells are endowed with lower proteasome pools, we measured the levels of catalytic β-subunits by immunoblotting. Being subjected to autocatalytic cleavage upon assembly to generate the active form, the steady-state levels of mature β-subunits provide a measurement of the actual proteasome capacity 26. Immuno-proteasomes are believed to represent the the majority of cellular proteasomes, and the main extra-lysosomal proteolytic system in lymphoid organs, in particular in the B cell lineage 22,27,28. Indeed, while the steady-state levels of constitutive catalytic subunits do not change significantly between the lines (not shown), we found that all three immuno-catalytic subunits (LMP2, LMP7 and MECL-1) are significantly lower in MM.1S and KMS.18 cells than RPMI8226 and U266 cells (Fig. 2B). Therefore, MM.1S and KMS.18 cells, the most PI-sensitive lines, express a smaller proteasome complement, accounting for reduced overall proteasome activity. Conversely, the steady-state levels of □subunits, which do not report on assembled, functional proteasomes 26 were similar in the 4 MM lines (Fig. 2B). Immunofluorescence for LMP2 (not shown) or LMP7 confirmed higher general levels

of immunoproteasomes in U266 as compared to MM.1S cells (Fig. 2C). Altogether, these findings reveal that different myelomas may be equipped with different levels of assembled, functional proteasomes, indicating a potential molecular mechanism contributing to variable susceptibility to PI. *Increased proteasomal workload in PI-sensitive MM cells*

We next asked whether MM lines cells also differ in the actual use of the proteasomal degradative route. In several independent pulse-chase assays, the amount of proteasomal degradation of newly synthesized proteins was significantly higher in KMS.18 and MM.1S than RPMI8226 or U266 cells (Fig. 2D, left panel). Moreover, in a 5 min pulse, KMS.18 and MM.1S incorporated 3-4 times more radioactivity than RPMI8226 or U266 cells into TCA-insoluble polypeptides, indicative of higher protein synthesis (Fig. 2D, right panel), but secreted ~half as much as U266 cells in 30 min chase (not shown). The observation that PI-sensitive MMC also rely more on proteasomal degradation suggests that proteasomal workload may contribute to determine the intrinsic sensitivity to PI of a neoplastic clone.

Critical proteasome stress in PI-sensitive MM cells

The combination of lower proteasome expression and higher workload in PI-sensitive MMC led us to predict profound biological differences between differentially sensitive MM lines. Thus, to address if PI-sensitive MMC suffer from proteasome stress, we assessed accumulation of poly-ubiquitinated proteins. Immunofluorescent staining revealed the presence of poly-ubiquitinated proteins in basal conditions in KMS.18 and MM.1S cells, with a discrete cytosolic pattern, exceeding the signal present in U266 or RPMI8226 cells (Fig. 3A). Immunoblot analyses confirmed higher poly-ubiquitinated proteins in MM.1S as compared to U266 cells, with parallel lower levels of free ubiquitin (Fig. 3B). 24hr treatment with increasing doses of bortezomib causes further accumulation of poly-Ub proteins in all lines, reaching comparable levels at the EC50 dose calculated at 48 hrs (Fig. 3A, bottom panels). To test if a critical level of proteasome overload precedes death, we exploited an unstable GFPfused to a mutated, uncleavable ubiquitin moiety driving poly-ubiquitination and rapid proteasome-mediated degradation (UbG76V-GFP), an established reporter of proteasome overload 13,29. By lentiviral transduction, we engineered MM lines to stably express UbG76V-GFP. Despite differential basal efficiency of the ubiquitin proteasome system in U266 and MM.1S cells (Fig. 3A-B), basal UbG76V-GFP was comparable in the two cell lines, and accumulated upon pharmacological proteasome blockade, as assessed by FACS (Fig. 3C). Importantly, PI sensitivity of engineered MM lines was comparable to that of wild-type cells, with MM.1S proving ~ten times more responsive than U266 cells both by GFP accumulation and in apoptosis assays (not shown). Treatment of UbG76V-GFP expressing U266 and MM.1S cells with increasing doses of bortezomib demonstrated a critical proteasomal overload upon 24 hr treatment at doses that differed by a factor 10 between the 2 lines, 24 hrs prior to cell death (Figs 3D-E). Altogether, these data further confirm a lower efficiency of the ubiquitin-proteasome system in PI-vulnerable MM cells. As a result, critical proteasomal overload levels precede PI-induced death.

Increasing workload through ER stressors sensitizes MM cells to PI

We next aimed at determining whether proteasome activity and workload are causally linked to apoptotic sensitivity to PI in MMC. To this aim, we manipulated either parameter before measuring PI sensitivity. To increase proteasome load we used drugs known to induce protein misfolding in the ER (e.g. the N-glycosylation inhibitor tunicamycin, Tm) and to activate the unfolded protein response (UPR) 30. To establish a solid assay, we selected a low dose of Tm (2,5 μg/ml) capable of inducing an UPR, as indicated by modest XBP-1 splicing after 24 hr of treatment (Fig. 4A, top

inserts), followed by negligible toxicity, as indicated by FACS analysis of apoptosis, at 48 hr (Fig. 4A, bottom panels). In combination with low, non-toxic doses of bortezomib, massive apoptosis ensued in both cell lines (Fig. 4A), revealing strong synergism. Similar results were obtained with different PI (MG-132 and epoxomicin) and ER stressors (thapsigargin, brefeldin A) (not shown). To establish if the capacity of ER stressors to sensitize MM lines to PI is due to enhanced proteasome workload, we utilized UbG76V-GFP engineered MM lines. In engineered U266 cells, Tm caused a modest UPR, which was greatly enhanced by addition of bortezomib (Fig. 4B, top insert). Importantly, combination of the 2 drugs caused proteasomal overload in striking synergism in 24 hr (Fig. 4B, bottom panel), followed by extensive cell death at 48 hr (Fig. 4C). Similar results were obtained in engineered MM.1S cells (not shown). Taken together, these findings suggest that proteasome workload is causally involved in determining PI sensitivity, possibly underlying the powerful synergy between PI and ER stressors against MMC.

Raising proteasome capacity increases MMC resistance to PI

We then asked whether a causal link exists between proteasome activity and apoptotic sensitivity to PI in MMC. To this aim, we exploited the postulated capacity of mammalian cells to induce proteasome biogenesis in response to increasing proteolytic demands (*proteasome stress response)* 31-33. Continuous proteasome inhibition was recently used to select PI-resistant cells expressing proteasome genes at higher levels in a Burkitt lymphoma cell line. This treatment took weeks and markedly induced apoptosis, thereby failing to establish a rigorous cause-effect relationship between PI sensitivity and proteasome activity, as other detoxification mechanisms may be selected 34. We thus searched for low, non-toxic doses of reversible PI capable of increasing proteasome expression in shorter time, enabling us to avoid selection of resistant clones and better appraise the direct effect of increased proteasome biogenesis on the apoptotic sensitivity to bortezomib. Moreover, to counteract unlikely detoxification strategies, we used two distinct PI of different classes to induce proteasome biogenesis (MG-132, a peptide aldehyde) and test PI sensitivity (bortezomib, a peptide boronate). U266 cells were treated with 1 nM MG-132 for 2 days, followed by 10 nM for 3 days, washed thoroughly, left untreated for 4 days, sampled for protein extracts, and assayed for apoptosis after 48 hr treatment with increasing doses of bortezomib. Attesting to successful induction of proteasome biogenesis, MG-132-pretreated (conditioned) cells displayed significant increases of all 3 proteasome peptidase activities as compared to vehicle-treated controls (Fig. 5A). Importantly, conditioned MMC proved remarkably more resistant to bortezomib than unconditioned controls both at 24 (not shown) and 48 hr (Fig. 5B), but not to UV-induced apoptosis (Fig. 5C). Further attesting to specific protection via upregulated proteasome expression, MG-132 treatment failed to induce a significant heat shock response (Fig. 5D). The data strongly suggest that total proteasomal capacity contributes to determine PI susceptibility in MMC.

Proteasome stress and PI sensitivity in patient-derived MMC

The findings that proteasome workload and capacity contribute to determine the apoptotic sensitivity to PI in MM lines prompted us to challenge our model in primary myelomas. We thus utilized MMC from newly diagnosed patients to investigate the relationship *ex vivo* between Ig synthesis, proteasome stress, and PI sensitivity. We purified MMC from bone marrow aspirates and combined immunofluorescence, FACS and enzymatic assays with specific fluorogenic peptides 13 to measure accumulation of poly-ubiquitinated proteins, Ig content, apoptotic sensitivity to bortezomib and proteasome activity. MMC display spontaneous accumulation of poly-ubiquitinated proteins, while CD138- cells accumulate poly-ubiquitinated proteins only upon treatment

with PI (Fig. 6A), and prove much more resistant (up to 300 times) to PI-induced apoptosis (not shown). Although variable in intensity, the presence of poly-ubiquitinated proteins coincides with plasma cell identity (certified by Ig expression, Fig. 6A-B). Moreover, the fluorescence intensity associated to poly-ubiquitinated proteins positively correlates with that of Ig-L within the MMC population of each patient analyzed (Fig. 6C), and among different patients (Fig. 6D), suggesting a role for Ig synthesis and/or retention in determining proteasome workload.
Finally, *in vitro* assessment of overall proteasome activity per total protein content revealed that, similar to MM lines, proteasome capacity varies among patients (ranging from ~0.2 to ~0.6 nM fluorogenic probe cleaved/ mg total protein/ min), as did the intrinsic apoptotic sensitivity to PI (the EC50 ranging from ~2 to ~20 nM bortezomib). Importantly, a direct correlation was evident between EC50 and proteasome capacity (Fig. 6E), strongly suggesting that the size of the proteasome compartment contributes to determine PI sensitivity also in primary MM.
Altogether, these data indicate a strong relationship between Ig synthesis and accumulation of poly-ubiquitinated proteins, a hallmark of proteasome stress. Single cell assays allowing to measure proteasome capacity and proteotoxic stress might prove useful to predict individual PI sensitivity and possibly customize MM therapy.

Discussion

To maintain homeostasis, cells activate adaptive strategies against stressful and potentially harmful conditions (e.g. hypoxia, nutrient deprivation, oxidative stress). On the other hand, stress duration and intensity can activate apoptotic escapes, turning these responses maladaptive 35. Due to deregulated growth, cancer cells generally experience more cytotoxic stress than normal counterparts, leading to constitutive activation of such responses 36-39, which may in turn confer a growth advantage and mediate resistance against cytotoxic insults, including drugs. Since physiological apoptotic responses to genotoxic stress are often disabled in cancer, strategies to increase cytotoxic stress offer great therapeutic promise to achieve cancer cell death through intact apoptotic programs 36.
Having established intriguing correlations between proteostasis and PI sensitivity in Ab secretors 13,14, we became interested in investigating whether proteotoxic stress may represent a therapeutic target against MM, the paradigmatic PI-responsive cancer. Not surprisingly, in view of their secretory origin, MMC display an active UPR, the pathway activated by the accumulation of misfolded/ unfolded peptides in the ER 17. In MM, increased expression of XBP-1s, a UPR component essential for plasma cell differentiation and function 40,41, correlates with bad prognosis and poor survival 42, and could directly contribute to MM pathogenesis 43. However, the role played by the UPR in MMC, and how PI affect it, is still controversial 44. Recently, the UPR required for differentiation and function of professional secretory cells has been distinguished from the ER stress response (ESR), in which selective branches of the UPR are activated upon acute ER stress. The ESR generally restores homeostasis, but under overwhelming stress it triggers apoptosis 30,45,46. The different toxicity of PI could depend on basal stress conditions and ongoing adaptive responses, including the UPR.
Given the key role of proteasomes in degrading unfolded/ misfolded proteins, we wondered if the exquisite sensitivity to bortezomib displayed by certain MMC could be, at least partially, explained by the high requirement for proteasome function. To test this hypothesis, we first exploited an established model of plasma cell differentiation characterized by a dramatic loss of proteasome expression associated

with acquisition of apoptotic sensitivity to PI 13,14. We found that, in addition to the reduced proteasome capacity, Ab-secreting cells also display a previously unreported increase in proteasomal workload, presumably due to metabolic stress associated with Ig synthesis (Fig. 1). An increased workload on fewer functional proteasomes generates an imbalance, predisposing to apoptosis 13. We then explored whether a similar imbalance underlies PI sensitivity in MMC. We first verified that 4 MMC with different sensitivity to bortezomib also have similar differential sensitivity to other PI, implying that the effectiveness of these drugs resides in specifically targeting the proteasome. Next, by assessing the level of proteasome activity with enzymatic and immunoblotting assays, we discovered that the most vulnerable cells, KMS.18 and MM.1S, indeed have fewer active proteasomes (Fig. 2). Collectively, our findings imply that different myelomas may be equipped with different levels of functional proteasomes, with reduced proteasome capacity correlating with high PI sensitivity. Together with reduced proteasomal activity, KMS.18 and MM.1S also display increased RDP production (Fig. 2D). This suggests that proteasomal workload is not constant, but can vary greatly, correlating with PI sensitivity in MMC. Thus, proteasome expression can be low despite elevated functional demands. Importantly, PI-sensitive MMC also display higher incorporation of radioactive amino acids into TCA-insoluble polypeptides, reflective of increased protein synthesis during the pulse. Thus, the work accomplished by each proteasome (as can be judged by dividing load by capacity) in PI-sensitive MMC is almost 2 logs higher than in relatively PIresistant MMC. Moreover, our pulse-chase assays showed that PI-sensitive MMC secreted fewer proteins, despite higher synthesis, as in a recent report showing increased ER retention of Ig components possibly causing PI sensitivity 17. Taken together, the data suggest that efficiency of protein synthesis is greatly reduced in KMS.18 and MM.1S cells, generating more side products requiring proteasomal degradation, but the increased demand is not matched by an upgrade of the proteasomal apparatus, leading to proteasome stress, in coincidence with exquisite PI sensitivity (Fig. 3). Interestingly, the observed basal accumulation of poly-Ub proteins in PI-sensitive MMC is compatible with normal cell functions and with degradation of an unstable Ub-GFP reporter, which proved useful to demonstrate critical proteotoxic levels and to unveil pharmacological synergies (Figures 3 and 4).

The obvious next question is whether an imbalance between proteasome workload and capacity is causally linked to the higher susceptibility to PI distinctive of certain myelomas. If this were the case, proteasome stress could be exploited to predict PI sensitivity. To address this question, we set out to modulate proteasome expression and functional workload in order to modify PI sensitivity. We successfully increased workload by means of ER stressors: tunicamycin, an inhibitor of N-linked glycosylation; thapsigargin, which disrupts ER calcium stores, and brefeldin A, a blocker of ER-Golgi transport. By increasing misfolded proteins in the ER, these drugs increase the requirement for proteasome degradation 30,47. As expected, the administration of non-toxic doses of these drugs induced a modest UPR, but in combination with non-toxic doses of PI synergistically triggered ER stress, proteasome overload, as revealed by accumulation of the unstable Ub-GFP reporter, and cell death (Fig. 4). Our finding that ER stressors strongly sensitize MMC to bortezomib-induced apoptosis are consistent with previous reports 17,44,48 and extend our earlier observation that inducible expression of orphan Ig-μ chains made nonlymphoid cells vulnerable to PI, linking ER load to PI sensitivity 13.

In MM lines, Ig synthetic levels correlated with PI sensitivity 16, raising the possibility that increased Ig side products may overload proteasomes and sensitize to PI 16. Our data prove this hypothesis correct, and demonstrate that proteasome workload may represent

an independent variable directly influencing PI sensitivity in MMC. This framework may help to increase responsiveness to PI, or to reduce PI doses and toxicity, and contribute to explain the synergistic effect of ER stressors and PI against MMC reported by others, and confirmed herein 44,48. Furthermore, our findings validate MM lines engineered to express UbG76V-GFP for potential preclinical drug screening.

We next tested if proteasome capacity *per se* modulates PI sensitivity. Eukaryotic cells can respond to decreased proteasome function or increased proteasomal requirement by enhancing proteasome biogenesis, thereby defining a *proteasome stress response* 31-33. We thus augmented proteasome activity by growing MMC in presence of low doses of MG-132, a rapidly reversible PI, for a few days. Importantly, our approach increased proteasomes without any overt toxicity, avoiding selection of high proteasome-expressing clones. Together with higher proteasome capacity, conditioned MMC acquire increased resistance to bortezomib, but not UV-induced apoptosis (Fig. 5), confirming that the size of the proteasome complement is a key determinant of PI sensitivity.

Although a recent study on more heterogeneous cell line panels yielded opposite correlations between levels of proteasome subunits and PI sensitivity 49, our findings clearly show that in MM, lower levels of functional proteasomes not only correlate, but may be causally involved in determining high PI sensitivity.

Our data are in line with a recent report that forced overexpression of the rate-limiting catalytic □5 subunit increased proteasome activity and resistance to cytotoxic insults in fibroblasts 50. Clearly, the development of acquired resistance to bortezomib may involve other mechanisms, including overexpression of mutated proteasome target subunits, not necessarily affecting overall proteasome activity 51.

Our results indicate that basal proteasome levels and function may vary greatly among different MMC, with profound implications for the intrinsic capability of coping with cytotoxic stress, given the key role of the proteasome in integrating signals that control cell cycle progression, apoptosis, and metabolism. We are aware that studying MMC prescinding from their natural bone marrow milieu may present limits. However, we found that incubation with patient-derived purified stromal components does not alter proteasome activity in MM lines, which maintain the observed differences (Supplementary Fig. 2).

At present, it is not known whether differential proteasome expression in MMC results from reduced subunit synthesis or/and proteasome assembly/ stability 26. The molecular mechanism mediating the proteasome stress response has been identified in yeast, but remains elusive in mammalian cells. We have recently shown that differentiating B cells decrease their proteasomes despite increasing proteolytic demands 13,14, and now provide evidence that certain MMC express inadequate proteasome levels. It could be that shortlived Ab-secreting cells and certain myelomas respond poorly to proteasome stress, becoming vulnerable to conditions challenging proteasome function. In this connection, it is worth mentioning that unlike U266 and RPMI8226 cells, MM.1S proved irresponsive to proteasome stress, failing to increase their proteasome content (not shown). Thus, B cell differentiation and MMC may provide powerful experimental models to investigate the mechanisms regulating the proteasome stress response in mammalian cells. It remains to be seen whether and how long-lived plasma cells homing in the bone marrow maintain a suitable *load vs. capacity* ratio 52.

The identification of symptoms of proteasome stress in PI-vulnerable MMC (Fig. 3) implies that simple cell-based assays could be designed to predict individual responsiveness. A similar predictor might help design customized therapies, avoiding unnecessary exposure to bortezomib and unfavorable side effects. Although we did not correlate clinical responsiveness with cellular features, we assessed the intrinsic sensitivity to PI *in vitro* in primary, patient-derived MMC, and measured accumulation of

poly-ubiquitinated proteins, Ig content, and overall proteasome capacity. We found that poly-ubiquitinated proteins mark specifically neoplastic plasma cells, and their levels correlate with Ig content within every tumor cell population and among different patients, suggesting a direct effect of Ig synthesis and/or retention on proteasome workload. Moreover, overall proteasome activity varies among primary tumors, showing an inverse correlation with intrinsic responsiveness to PI as assessed *ex vivo* (Fig. 6). These data prompt to validate the assessment of proteasome stress and capacity as potential predictors of individual responsiveness to bortezomib of both prognostic and therapeutic value.

In conclusion, our data strongly support a model in which the balance between the workload on the ubiquitin-proteasome system and overall proteasome capacity may be crucial in determining the intrinsic apoptotic sensitivity of MMC to PI (Fig. 6F). Moreover, manipulating proteasome workload and capacity may disrupt adaptive responses, enhance cytotoxic stress, and trigger apoptosis of MMC with high specificity. Our work provides the framework for future experiments aimed at identifying new targets and designing novel combination therapies against MM and potentially other 'stressable' cancers.

Acknowledgements.

This work was supported through grants from the Associazione Italiana per la Ricerca sul Cancro (AIRC), Cariplo (NoBEL project), Ministero della Sanità, MIUR (CoFin and Center of Excellence in Physiopathology of Cell Differentiation), and Telethon. We are indebted to Miriam Ascagni, Holger Auner, Elisa Benasciutti, Elena Bois, Federico Caligaris-Cappio, Fabio Ciceri, Salvatore De Vita, Marina Ferrarini, Anna Fra, Alfred L. Goldberg, David Lomas, Elisabetta Mariani, Silvia Masciarelli, Giampaolo Merlini, Nir Netzer, Giulia Perrone, Luca Rampoldi, Aldo Roccaro, Keiji Tanaka, Jonathan Yewdell, Larry Wrabetz and Enzo Zimarino for scientific discussion, reagents and precious technical advice. We are thankful to Raffaella Brambati and Ana Fella for cheerful secretarial support. We apologize with our colleagues whose work was not cited owing to space limitations.

Authorship

Contribution: G.B., L.O. and P.C. designed, performed, and analyzed experiments and drafted the manuscript; N.P., A.O., F.F., E.P., A.M., and F.C. performed experiments and analyzed data; V.C., G.P. and N.G. provided clinical samples; K.C.A. provided general advice and critically reviewed the manuscript; R.S. and S.C. designed experiments, supervised the work, and wrote the manuscript.

Conflict-of-interest disclosure: The authors declare no competing financial interests.

Figure legends

Figure 1. Increased proteasomal workload in differentiating B-lymphocytes is associated with higher apoptotic sensitivity to PI. A) Increased rapid protein degradation in LPS-stimulated B cells. I.29μ+ cells stimulated with LPS for 0 or 3 days were pulsed for 30 min with 35S aminoacids and chased for the indicated times, with or without MG-132 (2 μM). The data indicate the percentage of TCA-insoluble radioactivity whose disappearance was inhibited by MG-132 at any given time point, relative to the total radioactivity present at the end of the pulse (*$p<0.05$). B) Increased RDPs in LPS-stimulated B cells. I.29μ+ cells cultured for 0 or 3 days with LPS were pulsed for 10 min and chased for 15 min, with or without MG-132. The bars show the percentage of radioactive polypeptides degraded by proteasomes during

the chase (*p<0.05). C) Increased apoptotic sensitivity in LPS-stimulated I.29μ+ cells. Cells were stimulated for 3 days with LPS or left untreated, and then treated for 5 hr with the indicated concentrations of bortezomib (Btz). The proportion of apoptotic (AnnexinV+ propidium iodide-) cells was measured by FACS analysis. One of three representative experiments is shown.

Figure 2. Reduced proteasome activity and increased workload in PI-sensitive MMC. A) Proteasome activity in the relatively sensitive KMS.18 and MM.1S and the relatively resistant U266 and RPMI8226 lines. Proteasome-specific chymotryptic, trypsin-like, and caspase-like activities were assessed in cell extracts and expressed on a per protein basis. The histogram shows the relative quantification of all 3 activities within each line, and levels relative to the corresponding activity in U266 (*p<0.001). The average of at least 4 independent experiments (±SD) is shown. B) Proteasome □-catalytic and □subunits in MM lines. Extracts from U266, RPMI8226, KMS.18 and MM.1S cells were resolved by SDS-PAGE and blotted with Ab to different proteasome catalytic β and non-catalytic □subunits (one of three representative experiments). Equal protein amounts were loaded in each lane, with a background stable band serving as a loading control (bckgd). The right panel shows the relative densitometric quantification of catalytic β subunits in 3 independent experiments (average ±SD), upon correction by the band intensity of β-actin in the corresponding blot. C) Immunofluorescence against LMP7 in U266 and MM.1S cells reveals higher immunoproteasome levels in the relatively less sensitive U266 cells. D) Higher proteasome workload and protein synthesis in PI-sensitive MMC. U266, RPMI8226, KMS.18 and MM.1S cells were pulsed for 5 min with 35S aminoacids and chased for 30 minutes, with or without PI (lactacystin, bortezomib and epoxomicin, 2 μM each). Proteasome-mediated degradation of newly synthesized proteins was calculated as the percentage of TCA-insoluble radioactivity whose disappearance during the chase was inhibited by PI, relative to the total radioactivity present at the end of the pulse, as in Fig. 1. The left panel shows proteasomal degradation in all MM lines, while the right panel quantifies the proteosynthetic activity of each line as the incorporation of hot amino acids into TCA-insoluble polypeptides at the end of the pulse. An average of three independent experiments (±SD) is shown. *p<0.001.

Figure 3. Differential sensitivity to proteasome stress in MMC. A) Basal and PIinduced accumulation of poly-ubiquitinated proteins in MMC. Immunofluorescent staining of poly-Ub proteins in U266, RPMI8226, KMS.18 and MM.1S cells. Top panels: untreated cells. Bottom panels: cells treated with bortezomib (Btz) for 24 hrs at the corresponding EC50 dose (calculated at 48 hrs). One of 3 independent experiments is shown. Size bar: 10 μm. B) Accumulation of poly-ubiquitinated proteins and lower levels of free ubiquitin in PI-sensitive MMC. Extracts from U266 and MM.1S cells were blotted with anti-ubiquitin (Ub). Poly-Ub proteins are detected as a smear in a 10% gel, while free Ub is detected in an 18% gel. □-actin serves as a loading control. C) MM.1S and U266 were engineered to stably express UbG76V-GFP, an established in vivo reporter of proteasomal overload 13,23,29. FACS analysis of basal UbG76V-GFP expression and its accumulation upon 4 hr treatment with Btz (1 μM for U266 and 100 nM for MM.1S). D-E) UbG76V-GFP accumulation upon 24hr treatment reveals critical proteotoxicity levels. UbG76V-GFP engineered U266 and MM.1S were treated with increasing doses of Btz for up to 48 hrs. D) FACS analysis of GFP expression reveals massive accumulation of GFP upon 24 hr treatment in both MM.1S and U266 with 5 and 50 nM Btz respectively. E) Mean fluorescence intensity (MFI) at different doses reveals a critical accumulation of the reporter at 24 hrs (left

panel), 1 day prior to onset of apotosis (right panel).

Figure 4. Increasing proteasome workload through ER stress sensitizes MMC to PI. Pharmacological ER stressors increase proteasome workload and PI-induced cytotoxicity in MMC. A) FACS analysis of apoptosis upon treatment with tunicamycin (Tm 2.5 μg/ml) or bortezomib (Btz, 10 nM for U266 and 1 nM for MM.1S), alone or together for 48 hrs. Top inserts show the level of XBP-1 splicing after 24 hrs (*u* and *s* for unspliced and spliced, respectively). B) 24 hr treatment with Tm (2.5 μg/ml) and Btz (5 nM) synergistically causes ER stress (XBP-1 splicing, top insert) and accumulation of UbG76V-GFP (bottom overlay FACS histogram) in engineered U266 cells. C) 48 hr treatment with Tm and Btz triggers synergistic death of engineered U266 cells. Cell death was assessed by modifications of physical parameters by FACS. One representative experiment is shown.

Figure 5. Increasing proteasome expression specifically enhances resistance towards PI. U266 cells were treated for 5 days with low, non-toxic doses of MG-132 (2 days 1 nM followed by 3 days 10 nM). Cells were then washed and cultured in fresh media for 4 more days, and then assayed for overall proteasome activity and apoptotic sensitivity to bortezomib. A) Significant increases of proteasome-specific activities in MG-132-conditioned MMC. Conditioning treatment resulted in doubled chymotryptic and caspase-like activities, and □50% increase in trypsin-like activity. *$p<0.05$. B) Conditioned cells show enhanced PI resistance. MG-132-conditioned and vehicle-treated cells were exposed to the indicated doses of bortezomib (Btz) for 48 hrs, and apoptosis assessed by FACS as the proportion of AnnexinV+ propidium iodide- cells. The line graph averages (□SD) 2 representative experiments. $p<0.05$. C) Conditioned cells are not protected from UV-induced apoptosis. MG-132-conditioned and vehicle-treated cells were exposed to UV rays for the indicated times, and apoptosis assessed as above after 24 hrs. One representative experiment is shown. D) MG-132 conditioning treatment fails to induce a detectable heat shock response. MG-132-conditioned and vehicle-treated cells were sampled at the indicated days from the begenning of the treatment, and mRNA levels for inducible HSP70 quantitated by realtime RT-PCR. 1 hr exposure to 43°C (heat) significantly increased HSP70i mRNA in U266 and HeLa cells. One representative experiment is shown.

Figure 6. Proteasome stress predicts sensitivity of primary MMC to bortezomib. Primary, patient-derived MMC were selected by immunomagnetic purification from bone marrow biopsies and divided in 3 pools. The first pool was seeded onto polylysinated slides and assayed for accumulation of poly-Ub proteins and Ig light chain (Ig-L) expression by immunofluorescence. The second pool was plated in multiwall plates, challenged with increasing doses of bortezomib for 24 hr, and apoptotic responses assessed by highly sensitive FACS analysis (LSRII) upon labelling with conjugated AnnexinV and propidium iodide. The third pool was assayed *in vitro* for proteasome-specific chymotryptic activity by means of a specific fluorogenic peptide, as in Fig. 3. A) Spontaneous accumulation of poly-Ub proteins in primary MMC. While in the CD138- fraction poly-Ub proteins accumulate only upon treatment with PI (16 hr with 100 nM bortezomib, Btz, in the bottom left panel), CD138+ MMC (hallmarked by Ig-L expression) show Fk2+ fluorescence in basal conditions (2 representative cases shown). Images were deconvoluted with DeltaVision and SoftWorx; single z sections are shown. Size bars: 5 μm. B) Poly-Ub proteins are highly specific of Ig-L+ MMC. Automated quantification of fluorescence in Ig-L+ and Ig-L- nucleated cells was performed using a dedicated software (see Methods). The

box plot shows the average fluorescence intensity (FI), with 2.5 top and bottom percentiles; *p<0.001. C) Intra-patient positive correlation between poly-Ub accumulation and Ig-L content. Each dot corresponds to a single MM cell and each plot corresponds to one patient. Scatters from three representative patients are shown. r>0.6; p<0.0001. D) Positive correlation of poly-Ub protein accumulation and Ig-L content among different patients. MFI: mean fluorescence intensity. r=0,95; p<0.05. E) Primary MM endowed with high proteasome capacity are intrinsically less responsive to Btz. In 4 primary samples we measured overall proteasome activity in cell lysates by means of a fluorogenic peptide specifically probing the 26S chymotryptic activity (ZGGL-amc) 13,14. Proteasome-specific chymotryptic activity is expressed as nmoles probe cleaved per min per mg protein. Dose-response curves were generated by 24 hr treatments with Btz. To determine the intrinsic sensitivity of each MM clone, EC50 values were calculated using nonlinear regression with the Prism software (GraphPad). F) A model of proteasome-related determinants of apoptotic sensitivity to PI. Relatively PI-resistant MMC are equipped with high proteasome pools, both in absolute terms, and relative to degradative demands. As a result, few proteins await degradation, and high levels of free ubiquitin are available to target new proteasome substrates. In contrast, PI-sensitive MMC are equipped with poor proteasome levels, despite high metabolic demands. As a result, huge amounts of poly-Ub proteins accumulate upstream of overloaded proteasomes, and little ubiquitin is available for proteins to be degraded. Although cells are healthy, stresses that further challenge the ubiquitin-proteasome system will unveil a lower apoptotic threshold.

References

1. Kisselev AF, Goldberg AL. Proteasome inhibitors: from research tools to drug candidates. Chem Biol. 2001;8:739-758.
2. Kuehl WM, Bergsagel PL. Multiple myeloma: evolving genetic events and host interactions. Nat Rev Cancer. 2002;2:175-187.
3. Adams J. The proteasome: a suitable antineoplastic target. Nat Rev Cancer. 2004;4:349-360.
4. Richardson PG, Sonneveld P, Schuster M, et al. Extended follow-up of a phase 3 trial in relapsed multiple myeloma: final time-to-event results of the APEX trial. Blood. 2007;110:3557-3560.
5. Rajkumar SV, Richardson PG, Hideshima T, Anderson KC. Proteasome inhibition as a novel therapeutic target in human cancer. J Clin Oncol. 2005;23:630-639.
6. Richardson PG, Barlogie B, Berenson J, et al. Clinical factors predictive of outcome with bortezomib in patients with relapsed, refractory multiple myeloma. Blood. 2005;106:2977-2981.
7. Mulligan G, Mitsiades C, Bryant B, et al. Gene expression profiling and correlation with outcome in clinical trials of the proteasome inhibitor bortezomib. Blood. 2007;109:3177-3188.
8. Goldberg AL. Protein degradation and protection against misfolded or damaged proteins. Nature. 2003;426:895-899.
9. Glotzer M, Murray AW, Kirschner MW. Cyclin is degraded by the ubiquitin pathway. Nature. 1991;349:132-138.
10. Zhao J, Tenev T, Martins LM, Downward J, Lemoine NR. The ubiquitinproteasome pathway regulates survivin degradation in a cell cycle-dependent manner. J Cell Sci. 2000;113 Pt 23:4363-4371.

11. Anderson KC. Moving disease biology from the lab to the clinic. Cancer. 2003;97:796-801.
12. Yewdell JW, Reits E, Neefjes J. Making sense of mass destruction: quantitating MHC class I antigen presentation. Nat Rev Immunol. 2003;3:952-961.
13. Cenci S, Mezghrani A, Cascio P, et al. Progressively impaired proteasomal capacity during terminal plasma cell differentiation. Embo J. 2006;25:1104-1113.
14. Cascio P, Oliva L, Cerruti F, et al. Dampening Ab responses using proteasome inhibitors following in vivo B cell activation. Eur J Immunol. 2008;38:658-667.
15. Neubert K, Meister S, Moser K, et al. The proteasome inhibitor bortezomib depletes plasma cells and protects mice with lupus-like disease from nephritis. Nat Med. 2008;14(7):748-755.
16. Meister S, Schubert U, Neubert K, et al. Extensive immunoglobulin production sensitizes myeloma cells for proteasome inhibition. Cancer Res. 2007;67:1783-1792.
17. Obeng EA, Carlson LM, Gutman DM, Harrington Jr WJ, Lee KP, Boise LH. Proteasome inhibitors induce a terminal unfolded protein response in multiple myeloma cells. Blood. 2006;107(12):4907-4916.
18. Markovina S, Callander NS, O'Connor SL, et al. Bortezomib-resistant nuclear factor-kappaB activity in multiple myeloma cells. Mol Cancer Res. 2008;6:1356-1364.
19. Cascio P, Call M, Petre BM, Walz T, Goldberg AL. Properties of the hybrid form of the 26S proteasome containing both 19S and PA28 complexes. Embo J. 2002;21:2636-2645.
20. Santoni de Sio FR, Cascio P, Zingale A, Gasparini M, Naldini L. Proteasome activity restricts lentiviral gene transfer into hematopoietic stem cells and is down-regulated by cytokines that enhance transduction. Blood. 2006;107:4257-4265.
21. Cerruti F, Martano M, Petterino C, et al. Enhanced expression of interferongamma-induced antigen-processing machinery components in a spontaneously occurring cancer. Neoplasia. 2007;9:960-969.
22. Cascio P, Hilton C, Kisselev AF, Rock KL, Goldberg AL. 26S proteasomes and immunoproteasomes produce mainly N-extended versions of an antigenic peptide. Embo J. 2001;20:2357-2366.
23. Neefjes J, Dantuma NP. Fluorescent probes for proteolysis: tools for drug discovery. Nat Rev Drug Discov. 2004;3:58-69.
24. van Anken E, Romijn EP, Maggioni C, et al. Sequential waves of functionally related proteins are expressed when B cells prepare for antibody secretion. Immunity. 2003;18:243-253.
25. Goldberg AL, Cascio P, Saric T, Rock KL. The importance of the proteasome and subsequent proteolytic steps in the generation of antigenic peptides. Mol Immunol. 2002;39:147-164.
26. Schmidt M, Kloetzel PM. Biogenesis of eukaryotic 20S proteasomes: the complex maturation pathway of a complex enzyme. Faseb J. 1997;11:1235-1243.
27. Eleuteri AM, Kohanski RA, Cardozo C, Orlowski M. Bovine spleen multicatalytic proteinase complex (proteasome). Replacement of X, Y, and Z subunits by LMP7, LMP2, and MECL1 and changes in properties and specificity. J Biol Chem. 1997;272:11824-11831.
28. Noda C, Tanahashi N, Shimbara N, Hendil KB, Tanaka K. Tissue distribution of constitutive proteasomes, immunoproteasomes, and PA28 in rats. Biochem Biophys Res Commun. 2000;277:348-354.
29. Dantuma NP, Lindsten K, Glas R, Jellne M, Masucci MG. Short-lived green

fluorescent proteins for quantifying ubiquitin/proteasome-dependent proteolysis in living cells. Nat Biotechnol. 2000;18:538-543.
30. Schroder M, Kaufman RJ. The mammalian unfolded protein response. Annu Rev Biochem. 2005;74:739-789.
31. Meiners S, Heyken D, Weller A, et al. Inhibition of proteasome activity induces concerted expression of proteasome genes and de novo formation of Mammalian proteasomes. J Biol Chem. 2003;278:21517-21525.
32. Lundgren J, Masson P, Mirzaei Z, Young P. Identification and characterization of a Drosophila proteasome regulatory network. Mol Cell Biol. 2005;25:4662-4675.
33. Hanna J, Finley D. A proteasome for all occasions. FEBS Lett. 2007;581:2854-2861.
34. Fuchs D, Berges C, Opelz G, Daniel V, Naujokat C. Increased expression and altered subunit composition of proteasomes induced by continuous proteasome inhibition establish apoptosis resistance and hyperproliferation of Burkitt lymphoma cells. J Cell Biochem. 2008;103:270-283.
35. Rutkowski DT, Kaufman RJ. That which does not kill me makes me stronger: adapting to chronic ER stress. Trends Biochem Sci. 2007;32:469-476.
36. Ma Y, Hendershot LM. The role of the unfolded protein response in tumour development: friend or foe? Nat Rev Cancer. 2004;4:966-977.
37. Mathew R, Karantza-Wadsworth V, White E. Role of autophagy in cancer. Nat Rev Cancer. 2007;7:961-967.
38. Moenner M, Pluquet O, Bouchecareilh M, Chevet E. Integrated endoplasmic reticulum stress responses in cancer. Cancer Res. 2007;67:10631-10634.
39. Dang CV, Kim JW, Gao P, Yustein J. The interplay between MYC and HIF in cancer. Nat Rev Cancer. 2008;8:51-56.
40. Reimold AM, Iwakoshi NN, Manis J, et al. Plasma cell differentiation requires the transcription factor XBP-1. Nature. 2001;412:300-307.
41. Iwakoshi NN, Lee AH, Vallabhajosyula P, Otipoby KL, Rajewsky K, Glimcher LH. Plasma cell differentiation and the unfolded protein response intersect at the transcription factor XBP-1. Nature immunology. 2003;4:321-329.
42. Nakamura M, Gotoh T, Okuno Y, et al. Activation of the endoplasmic reticulum stress pathway is associated with survival of myeloma cells. Leuk Lymphoma. 2006;47:531-539.
43. Carrasco DR, Sukhdeo K, Protopopova M, et al. The differentiation and stress response factor XBP-1 drives multiple myeloma pathogenesis. Cancer Cell. 2007;11:349-360.
44. Lee AH, Iwakoshi NN, Anderson KC, Glimcher LH. Proteasome inhibitors disrupt the unfolded protein response in myeloma cells. Proc Natl Acad Sci U S A. 2003;100:9946-9951.
45. Wu J, Kaufman RJ. From acute ER stress to physiological roles of the Unfolded Protein Response. Cell Death Differ. 2006;13:374-384.
46. Boyce M, Yuan J. Cellular response to endoplasmic reticulum stress: a matter of life or death. Cell Death Differ. 2006;13:363-373.
47. Davenport EL, Moore HE, Dunlop AS, et al. Heat shock protein inhibition is associated with activation of the unfolded protein response pathway in myeloma plasma cells. Blood. 2007;110:2641-2649.
48. Gu H, Chen X, Gao G, Dong H. Caspase-2 functions upstream of mitochondria in endoplasmic reticulum stress-induced apoptosis by bortezomib in human myeloma cells. Mol Cancer Ther. 2008;7:2298-2307.
49. Busse A, Kraus M, Na IK, et al. Sensitivity of tumor cells to proteasome inhibitors is associated with expression levels and composition of proteasome

subunits. Cancer. 2008;112:659-670.
50. Chondrogianni N, Tzavelas C, Pemberton AJ, Nezis IP, Rivett AJ, Gonos ES. Overexpression of proteasome beta5 assembled subunit increases the amount of proteasome and confers ameliorated response to oxidative stress and higher survival rates. J Biol Chem. 2005;280:11840-11850.
51. Oerlemans R, Franke NE, Assaraf YG, et al. Molecular basis of bortezomib resistance: proteasome subunit beta5 (PSMB5) gene mutation and overexpression of PSMB5 protein. Blood. 2008;112:2489-2499.
52. Manz RA, Hauser AE, Hiepe F, Radbruch A. Maintenance of serum antibody levels. Annu Rev Immunol. 2005;23:367-386.

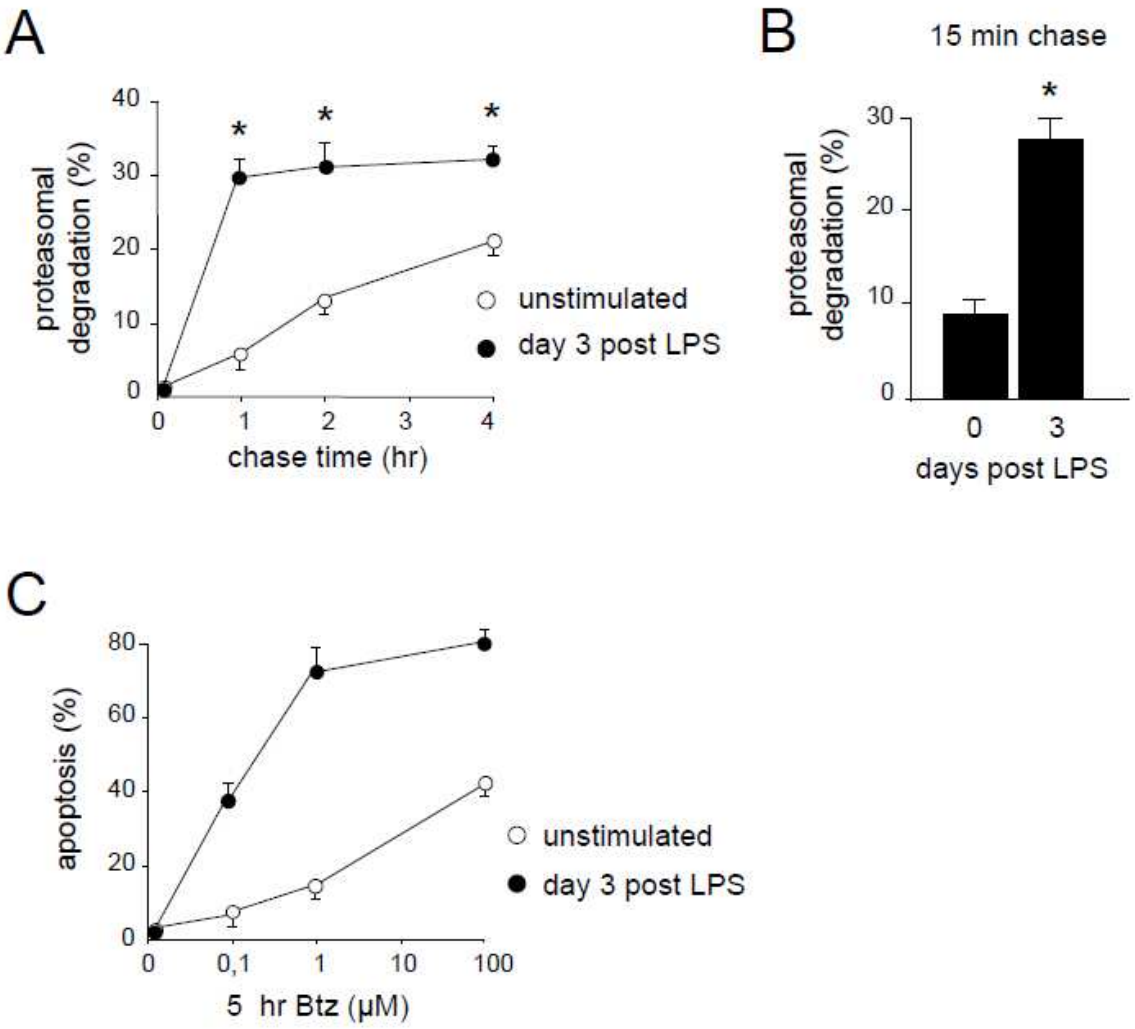

Bianchi et al, Figure 1

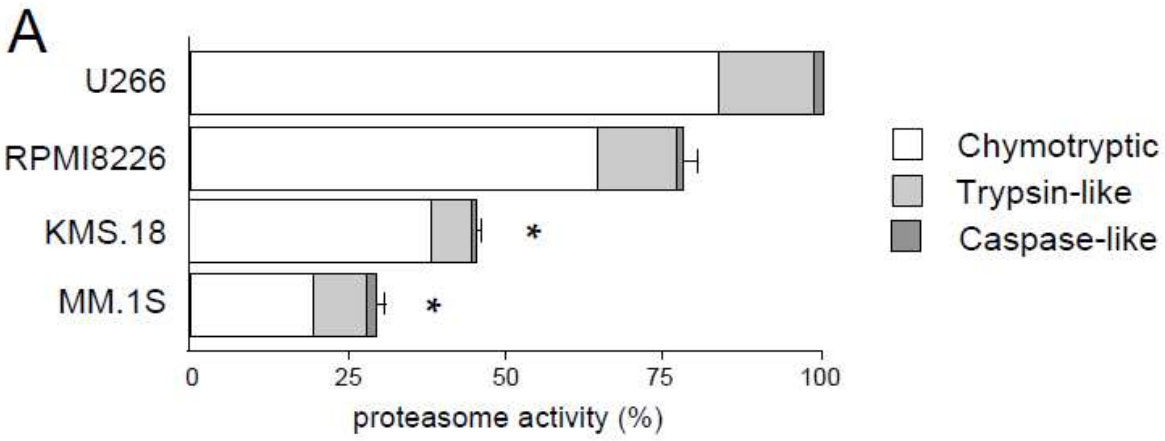

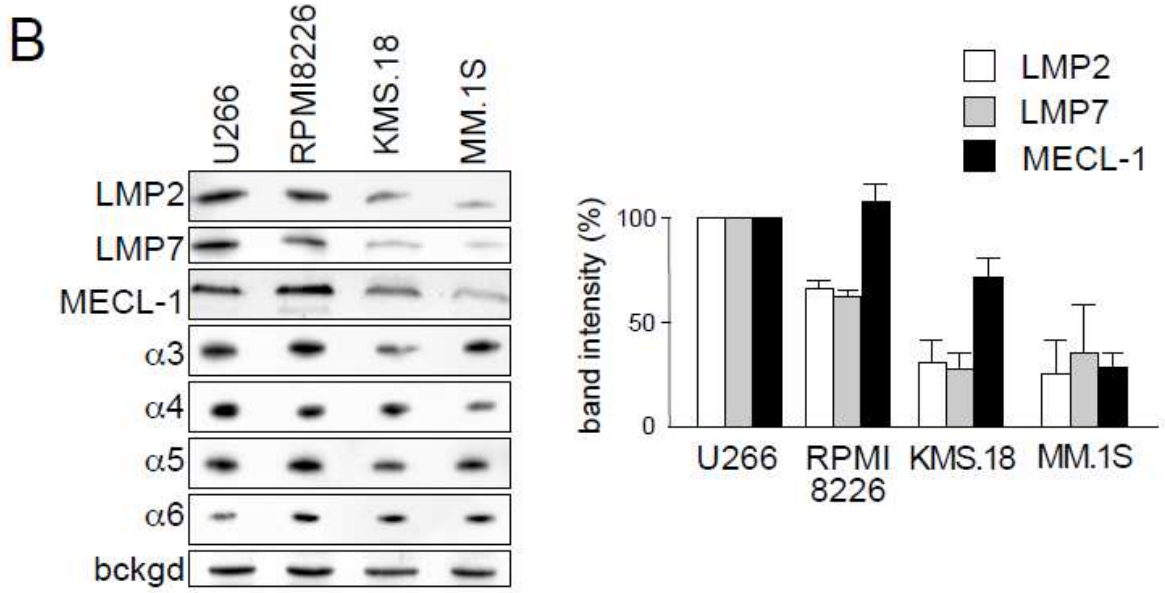

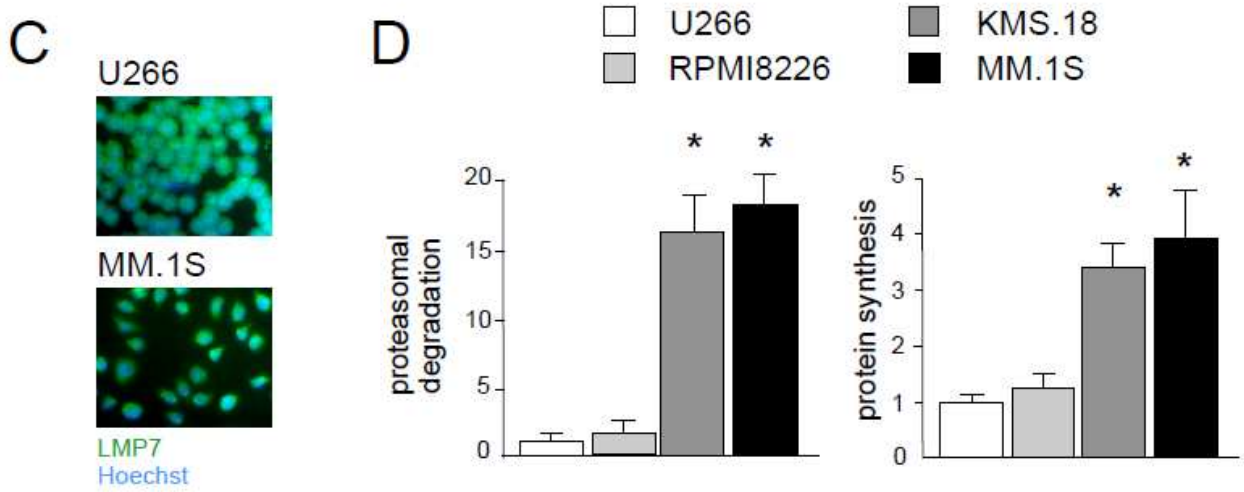

Bianchi et al, Figure 2

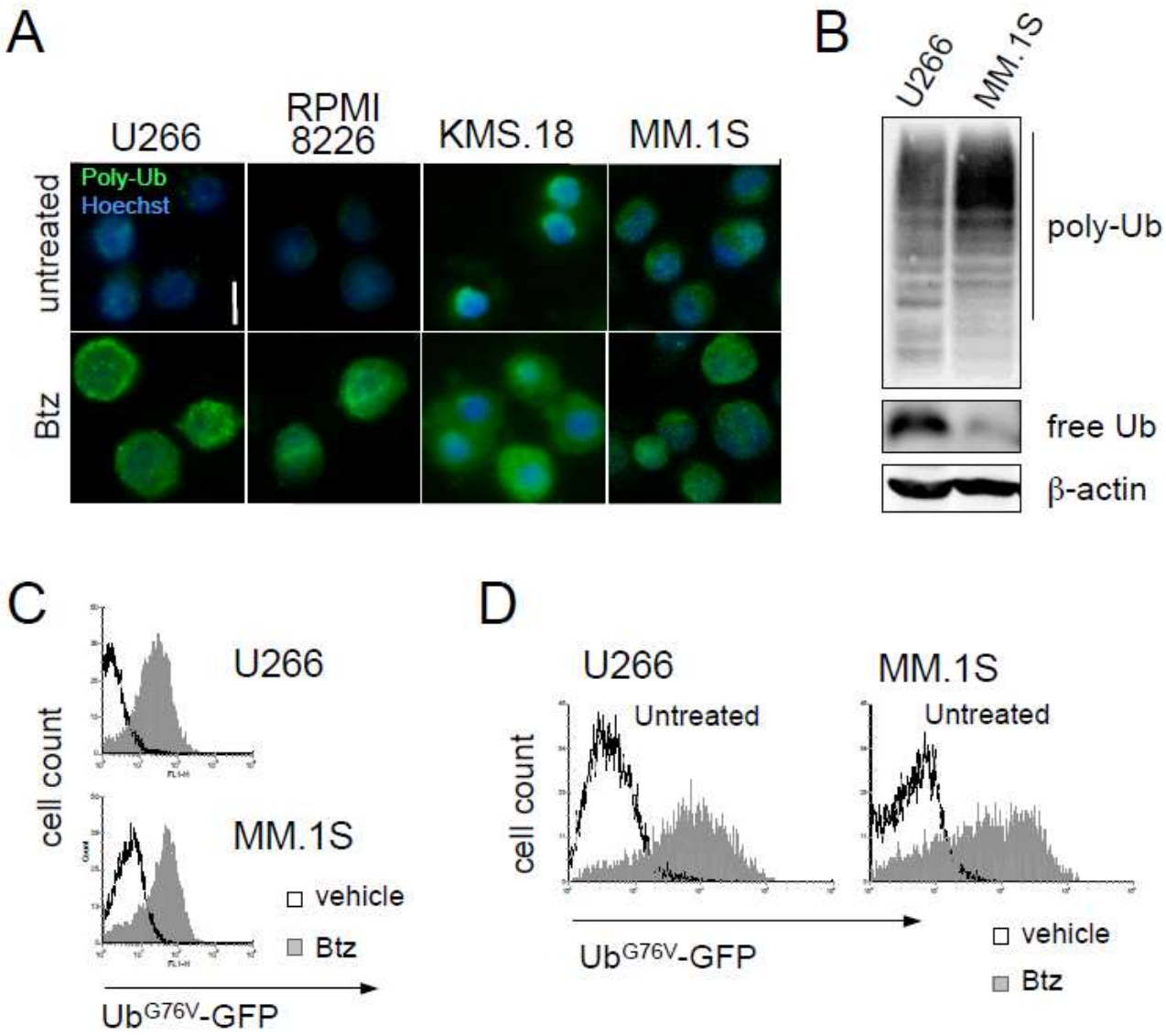

Bianchi et al, Figure 3

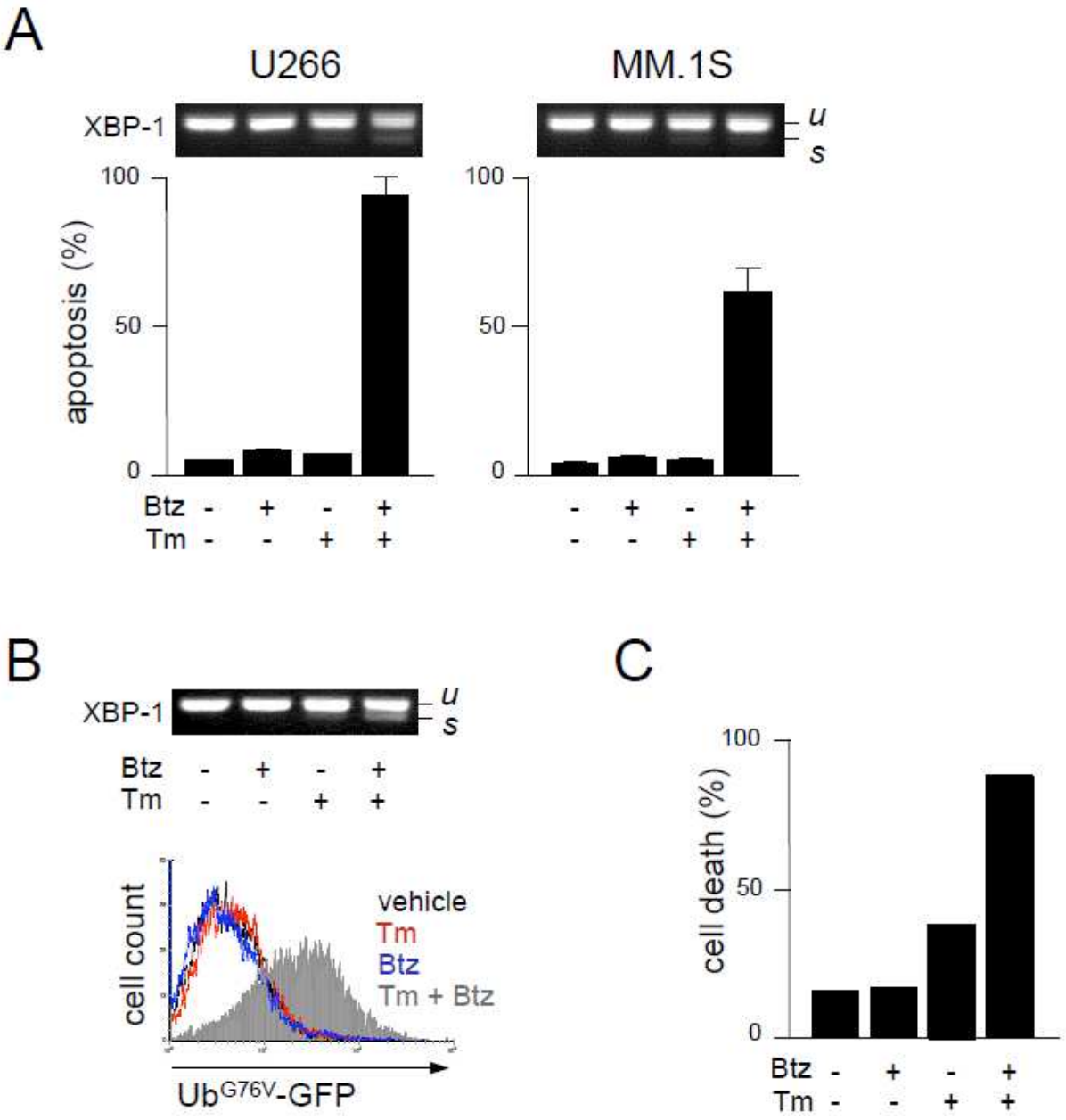

Bianchi et al, Figure 4

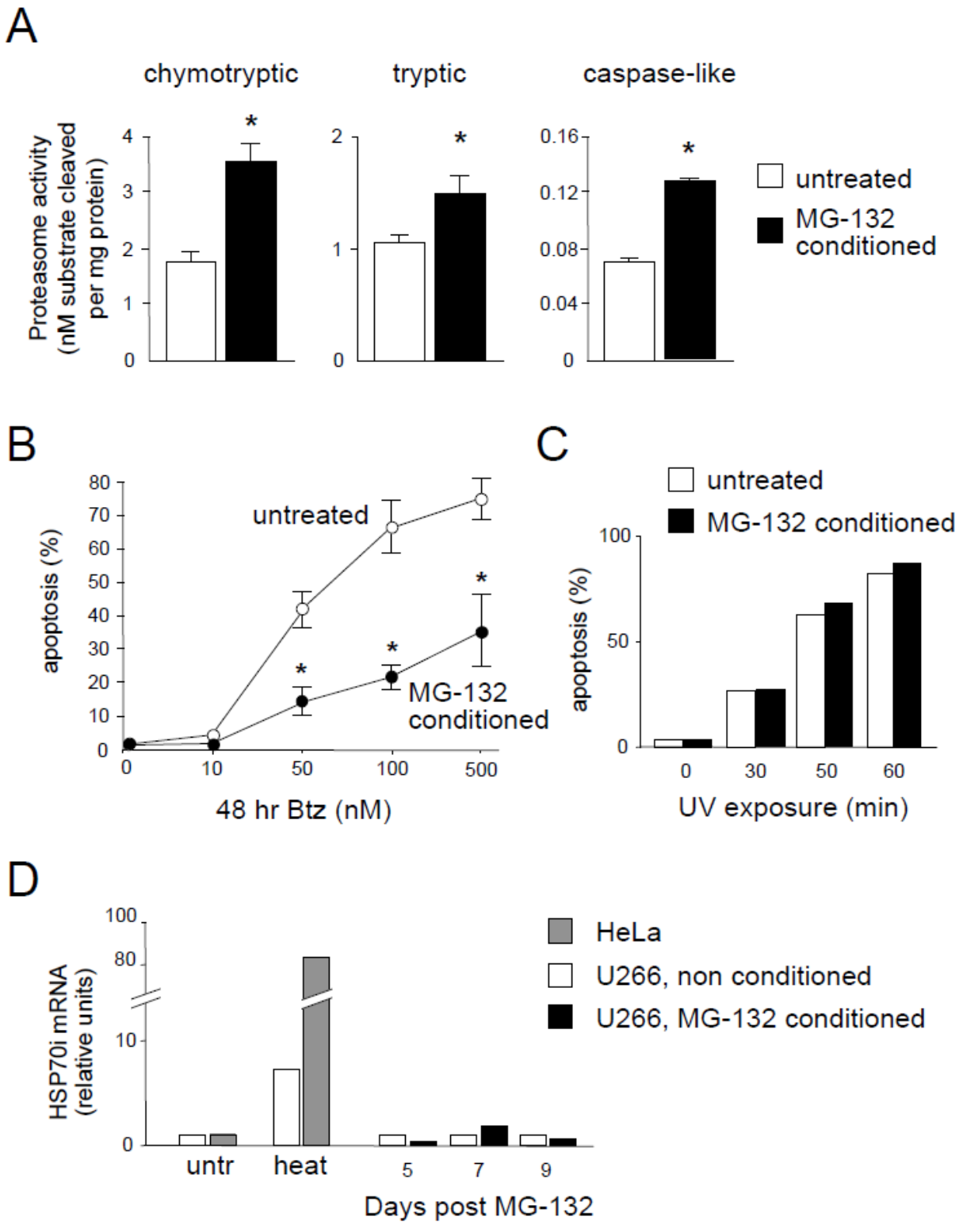

Bianchi et al, Figure 5

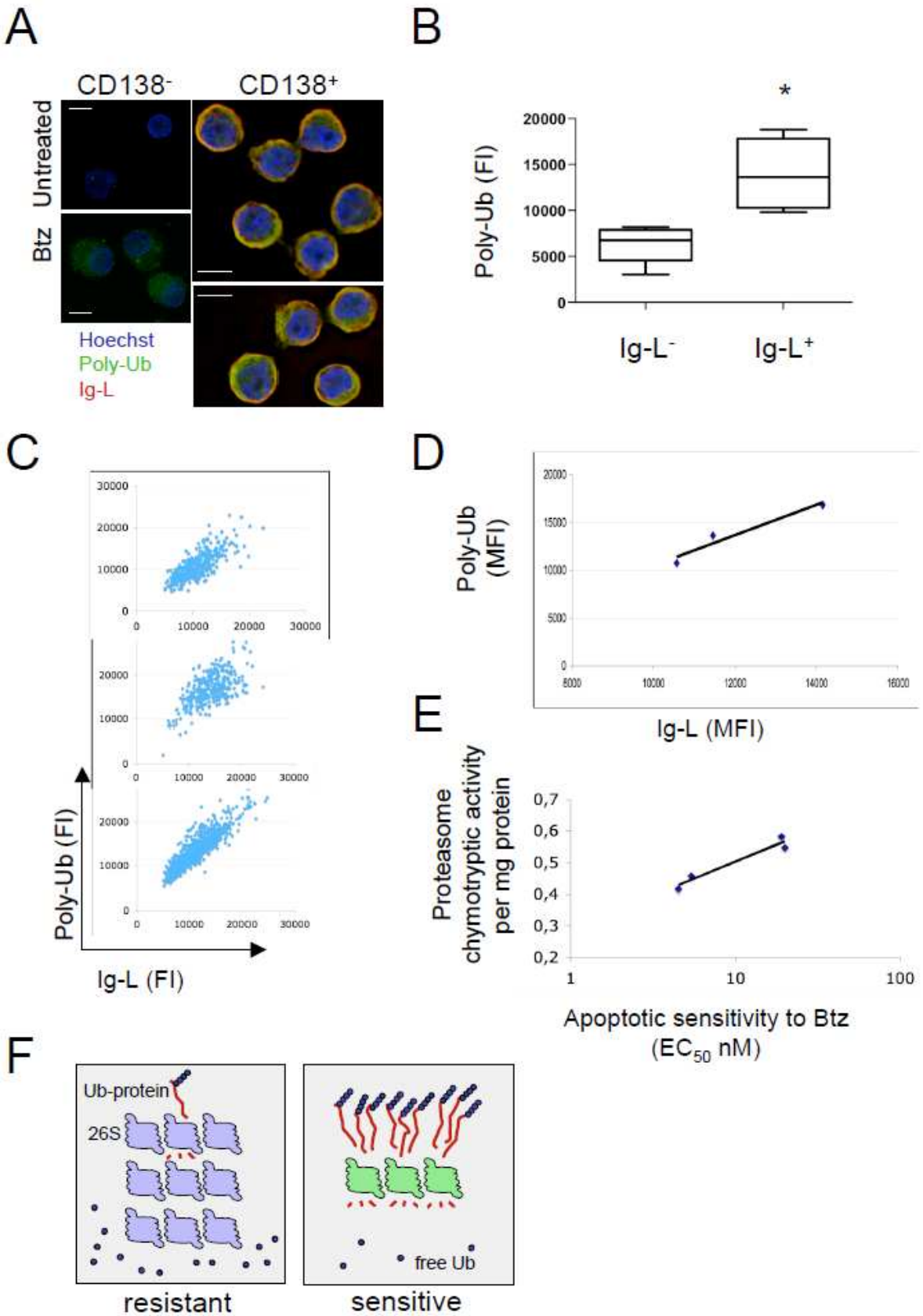

Bianchi et al, Figure 6